Unsteady laminar flow over a rough surface

T.G. MYERS

Dept of Mathematics and Applied Mathematics, University of Cape Town, Rondebosch 7701, Cape Town, South Africa (e-mail: myers@maths.uct.ac.za)

Abstract. A model is developed for the unsteady laminar flow of a thin fluid film over a substrate with roughness of the same order as the film height. The limits of large and small surface resistance and small surface-roughness are investigated and it is shown that at leading order the classical parabolic form for the velocity profile is retrieved in all cases. Empirical expressions for the depth-averaged velocity and the ratio of the average to maximum velocities are investigated and shown to agree with the present theory under certain conditions. The method is verified by comparison with experiments for steady uni-directional flow over a surface of known roughness.

Key words: laminar flow, rough surface, thin film

1. Introduction

Flow over surfaces where the roughness is of the same order as the fluid height may be separated into three distinct flow regimes; turbulent, transitional and laminar. The transition between the three flow regimes occurs, approximately, when the Reynolds number Re = 2000 and 500 [1, 2]. Turbulent flow is the most common in practical situations and has been studied intensively both experimentally and theoretically (see, for example, [3, 4]). Results for transitional flow are given in [5, 6]. At sufficiently low Reynolds number the flow around and above the roughness elements will be laminar; see [7, 8]. This is the least studied region for flow over a very rough surface and will form the focus of the current paper.

The two applications motivating this work are water flow over soil and accreting ice surfaces. Understanding flow over soil is important for a number of reasons, for example in modelling erosion, the movement of bacteria and fertiliser; see [9, 10]. Although turbulent flow is the most common situation in overland flow, laminar flow may also occur. Accreting ice surfaces are of particular interest to aircraft manufacturers, shipping and power transmission industries [11–13]. In aircraft applications the water flowing over the rough ice surface will form a very thin layer, with icing on structures the water flow is generally slow. In both cases laminar flow is likely to be the dominant form of water motion.

In this paper a theoretical model will be developed to predict laminar flow over a rough surface. Clearly, the fluid velocity will vary considerably depending on a fluid-particles position relative to the surface roughness elements. For example, the velocity will be lower in the vicinity of a peak in the substrate and higher over a smooth section; see [2], [7, Figure 7]. The velocity employed in the following analysis should therefore be considered as an average over a control area (not to be confused with the average velocity across the film, u_a). This will lead to inaccuracies on a local scale but should provide a reasonable approximation over a sufficiently large area. This approach has been verified experimentally in a study of flow on tidal flats and overland flow [14]. During the derivation it will be assumed that the film height

is greater than the roughness height, *i.e.*, $h > k$. It is a simple matter to adapt the analysis to situations where $h < k$. However, no appropriate experiments have been found to validate this limit and so this work focusses only on situations where $h > k$.

Previous theoretical models have dealt with laminar flow over relatively small surface roughness elements. One approach is to impose a no-slip boundary condition on a substrate with random roughness and then repeat the calculations to find a converged solution; see [15]. Using an alternative approach [16] shows that the standard no-slip velocity condition on the solid substrate, $u = 0$, may be replaced by a Navier slip condition

$$u = -\alpha \frac{\partial u}{\partial z}. \tag{1}$$

The slip coefficient, α, is the average roughness height. A similar condition was proposed in [17] by using an analogy with flow over porous media. However, this approximation is only valid in the limit $\alpha/h \to 0$, where h is the film height. In the present study the ratio α/h is non-negligible and applying this condition leads to significant negative velocities near the substrate. The slip condition is therefore not appropriate when the roughness has the same order of magnitude as the film height. There is also a body of work which considers in detail the flow over a single roughness element or obstacle; see, for example, [18, 19] and references therein. These models correctly capture the local physics but are not practical for dealing with flow over many roughnes elements.

In experimental studies of flow over a very rough surface two main techniques have been employed. In the first dye is introduced into the flow and the front of the plume tracked either visually or with a fluorometer [2]. In the second, saline solution is introduced and the plume position monitored by measuring the conductivity [3]. With both methods it is simplest to measure the maximum velocity, u_m. The average velocity is then estimated via a correction factor β, where $u_a = \beta u_m$; see, for example, [5]. In laminar flow over a smooth surface $\beta = 2/3$; in flow over a rough surface empirical estimates are required. Experimental heights are frequently inferred from $h = Q/u_a$, where Q is the known fluid flux/unit width. Errors in the estimation of u_m or β will therefore be reflected in an inaccurate prediction for the film height.

In laminar flow conditions the average velocity of a thin layer of fluid on a solid surface is

$$u_a = \frac{8gh^2 \sin\theta}{K\nu}, \tag{2}$$

where θ is the angle of inclination and ν the kinematic viscosity [20]. This is the appropriate form of the Darcy-Weisbach equation for flow in a wide channel. The coefficient $K = 24$ for flow over a smooth surface and increases as the roughness increases [21]. In reality K is an unknown function of u_a and Equation (2) is therefore impractical for predicting the average velocity [22]. The determination of β and K are therefore questions of practical interest.

A series of experiments for laminar, transitional and turbulent flow over a rough surface are described in [23]. Film heights and velocities are obtained via the saline technique. In the transitional and turbulent regimes the saline mixes well with the bulk fluid. In the laminar regime the saline falls to the bottom and so the measured velocities are below the true values. In [24] a model is developed for steady, uni-directional flow on a rough surface. Results are presented and compared with existing experimental results and a number of approximate empirical formulae. When comparing with results obtained via the saline technique, it is shown that the reported film heights are beyond the possible range for laminar flow and the saline
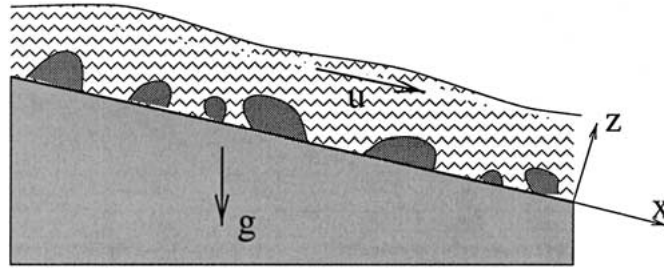
Figure 1. Schematic of problem showing a thin fluid film (length-scale ≫ height-scale) flowing over surface roughness elements

technique is therefore inappropriate for measuring laminar flow. This is described in more detail in Section 3.4.

A more complex study of the laminar flow regime was carried out by Phelps [7]. In this work small aluminium spheres (of diameter less than 0·025mm) were introduced into the water. The particles were viewed through a rotating prism with the aid of a microscope. This effectively provided a strobe system where the particle velocities could be related to the rotational speed. The depth of the particles was determined by the depth of focus of the microscope. This method allows velocity profiles, $u(z)$, and height to be accurately determined. It is clearly impractical for field trials, but it does provide excellent results for comparison with analytical and other experimental methods. Typically the results of Phelps indicate steeper velocity profiles than for smooth flow and $\beta \in [0·54, 0·65]$ for Re $\in [36, 500]$. In Section 5 the current theory is tested against these experimental results.

Further experimental work on laminar flow over a rough surface may be found in [3, 5, 7, 8, 23, 25, 26]. Guy *et al.* [9] study sediment-laden laminar flow. Lawrence [4] summarises a number of experimental results covering turbulent, transitional and laminar flow.

In the following section the theoretical model is developed. As is standard for thin-film laminar flow, the problem reduces to solving a single equation for the film height. Expressions for the fluid velocity and flux are obtained in terms of the film height, analytical expressions are then found for the average and maximum velocities. In Section 3, for large and small flow resistance, simple expressions for the velocity profiles, β and K are given and bounds for the steady-state film height are obtained. Velocity profiles are also compared with the theoretical model of Miksis and Davis [16]. In Section 5 the maximum velocity prediction is compared with the experimental results of Phelps.

2. Mathematical model

2.1. GOVERNING EQUATIONS

The problem configuration is shown in Figure 1. The fluid flows with velocity $\mathbf{u} = (u, v, w)$ under the action of gravity. The substrate is defined by the plane $z = 0$. The fluid has height h and the average roughness height is k. Provided the fluid flow is laminar and remains sufficiently thin, the Navier-Stokes equations may be approximated by

$$\frac{\partial^2 u}{\partial z^2} - f(u) = \frac{\partial p}{\partial x} - g_1 + \mathcal{O}(\epsilon^2, \epsilon^2 \text{Re}) = -\Lambda_1 + \mathcal{O}(\epsilon^2, \epsilon^2 \text{Re}) \tag{3}$$

$$\frac{\partial^2 v}{\partial z^2} - f(v) = \frac{\partial p}{\partial y} - g_2 + \mathcal{O}(\epsilon^2, \epsilon^2 \mathrm{Re}) = -\Lambda_2 + \mathcal{O}(\epsilon^2, \epsilon^2 \mathrm{Re}) \tag{4}$$

$$\frac{\partial p}{\partial z} \epsilon g_3 + \mathcal{O}(\epsilon^2, \epsilon^2 \mathrm{Re}) \tag{5}$$

The function f represents the resistance due to surface roughness; its specific form is discussed below. The dimensionless gravity components $(g_1, g_2, g_3) = (\hat{\mathbf{g}} \cdot \hat{\mathbf{x}}, \hat{\mathbf{g}} \cdot \hat{\mathbf{y}}, \hat{\mathbf{g}} \cdot \hat{\mathbf{z}})$, where $\hat{\mathbf{g}}$ is the unit vector in the direction of gravity. The terms Λ_i involve the pressure gradient and gravity. The pressure gradient acts to drive fluid spreading in the z-direction. On a flat surface this is the dominant driving force. However, on a slope it is typically an order of magnitude smaller than the gravitational force in the (x, y)-direction; see, for example, [27]. For completeness the pressure gradient in the x and y directions will be retained in the following analysis; however, in general it is negligible in comparison to g_1, g_2.

The variables are related to their dimensional counterparts by

$$x' = Lx \qquad y' = Ly \qquad z' = Hz = \epsilon Lz$$
$$u' = Uu \qquad v' = Uv \qquad w' = \epsilon Uw \tag{6}$$
$$p' = Pp \qquad t' = L/U \, t \,,$$

where dimensional terms are denoted with a prime. The height and length scales are H and L, the aspect ratio $\epsilon = H/L \ll 1$. The velocity scale $U = \rho g H^2/\mu$ is chosen so that gravity in the x- or y-direction balances the viscous resistance. On an almost horizontal surface the appropriate choice is $U = \rho g H^3/\mu L$ and the gravity term in (5) balances the pressure gradient. The pressure scale $P = \mu U/\epsilon^2 L$ is the standard one for lubrication theory.

Equations (3), (4) describe the velocity field. The terms on the left are the retarding forces, namely viscous resistance and resistance due to surface roughness, The terms on the right-hand side are the driving forces of pressure gradient and gravity. Above the roughness elements, $z > k$, $f = 0$. Within the rough region it is standard to assume that the resistance (or drag) to laminar flow is proportional to the square of velocity. In soil applications this is discussed in [4, 7]. This quadratic relation holds over a wide range of velocities. In the present study the velocity variation is relatively small, in which case the resistance may be well approximated by a linear relation, $f \approx \omega^2 u$, for an appropriate choice of resistance coefficient ω. The value of ω will depend on the amount and form of surface roughness and must be determined by comparison with experiments. The determination of ω and typical values are discussed in Section 5. In the following this linear relation between resistance and velocity will be imposed,

$$\begin{aligned} f(u) &= \omega^2 u, & 0 \le z \le k, \\ &= 0, & k \le z \le h. \end{aligned} \tag{7}$$

This simplification is the key to the following analysis. It permits analytical expressions to be obtained for the velocity, fluid flux and height. However, it should be borne in mind that such a simplification must limit the range of results; for example, if ω is determined from a given set of experiments over a range of velocities (or fluxes), care must be taken when using the analytical results for velocities (fluxes) outside of this range.

The fluid pressure may be determined by integrating Equation (5) to give

$$p = p_a + \epsilon g_3 (z - h), \tag{8}$$

where p_a is the ambient pressure and g_3 represents the gravitational component in the z-direction. The terms Λ_i may now be expressed as

$$\Lambda_1 = -\epsilon g_3 \frac{\partial h}{\partial x} - g_1 \tag{9}$$

$$\Lambda_2 = -\epsilon g_3 \frac{\partial h}{\partial y} - g_2. \tag{10}$$

The fluid velocity is obtained by integrating (3), (4) twice, after substituting for the resistance f from Equation (7) :

$$u = u_1 = a_1 \cosh \omega z + a_2 \sinh \omega z + \frac{\Lambda_1}{\omega^2}, \quad 0 \le z \le k,$$

$$= u_2 = -\Lambda_1 \frac{z^2}{2} + a_3 z + a_4, \quad\quad k \le z \le h, \tag{11}$$

$$u = v_1 = b_1 \cosh \omega z + b_2 \sinh \omega z + \frac{\Lambda_2}{\omega^2}, \quad 0 \le z \le k,$$

$$= v_2 = -\Lambda_2 \frac{z^2}{2} + b_3 z + b_4, \quad\quad k \le z \le h, \tag{12}$$

The constants of integration in (11) and (12) are determined by applying the following boundary conditions. At the substrate $z = 0$ there is no-slip, at the free surface $z = h$ there is no shear stress

$$u(0) = v(0) = 0, \quad \left.\frac{\partial u}{\partial z}\right|_{z=h} = \left.\frac{\partial v}{\partial z}\right|_{z=h} = 0. \tag{13}$$

At the interface between the two flow regions the velocity and shear stress must be continuous

$$[u] = [v] = 0, \quad \left[\frac{\partial u}{\partial z}\right] = \left[\frac{\partial v}{\partial z}\right] = 0, \tag{14}$$

where [ ] denotes the jump across the boundary $z = k$. In the following analysis, to avoid unnecessary repetition, only the x-components will be dealt with. The y-components can be obtained by substituting Λ_2 for Λ_1. Applying the boundary conditions leads to

$$a_1 = -\frac{\Lambda_1}{\omega^2}, \quad a_2 = \frac{-\Lambda_1}{\omega \cosh \omega k}(k-h) + \frac{\Lambda_1}{\omega^2}\tanh \omega k,$$

$$a_3 = \Lambda_1 h, \quad a_4 = -\frac{\Lambda_1}{\omega^2}\frac{1-\cosh \omega k}{\cosh \omega k} - \frac{\Lambda_1 k}{2}(2h-k) - \frac{\Lambda_1}{\omega}(k-h)\tanh \omega k.$$

The corresponding velocity is

$$u_1 = -\frac{\Lambda_1}{\omega^2}[\cosh(\omega z) - 1] - \frac{\Lambda_1}{\omega^2 \cosh(\omega k)}[\omega(k-h) - \sinh(\omega k)]\sinh(\omega z), \quad z \le k$$

$$u_2 = -\frac{\Lambda_1}{2}[(z-k)(z-k-2(h-k))] \quad\quad z \ge k \tag{15}$$

$$- \frac{\Lambda_1}{\omega^2 \cosh(\omega k)}(1 - \cosh(\omega k) + \omega(k-h)\sinh(\omega k)).$$

The velocity can be seen to depend on gravity (through Λ_1), the film and roughness heights and the resistance coefficient, ω. The velocity u_2 takes a classical parabolic profile. The second term on the right-hand side is a non-negative constant representing the velocity at the transition $z = k$.

Finally, provided the fluid is incompressible and w is continuous at the interface, $z = k$, the standard mass balance is

$$\frac{\partial h}{\partial t} + \nabla \cdot \mathbf{Q} = 0; \tag{16}$$

see [27] for further details. The flux $\mathbf{Q} = (Q_x, Q_y)$ is the integral of the velocity across the film,

$$Q_x = -\frac{\Lambda_1}{\omega^2} \left[\frac{\tanh(\omega k)}{\omega} - h + \frac{h - k}{\cosh(\omega k)} \right] - \frac{\Lambda_1}{3}(k - h)^3 -$$
$$\frac{\Lambda_1}{\omega^2 \cosh(\omega k)} \left[1 - \cosh(\omega k) + \omega(k - h)\sinh(\omega k) \right](h - k). \tag{17}$$

Hence the problem is governed by a quasilinear equation for the film height h.

When the system loses fluid, for example through evaporation or flow into the soil, or gains fluid through incoming droplets or condensation, the governing equation is modified to

$$\frac{\partial h}{\partial t} + \nabla \cdot \mathbf{Q} = E. \tag{18}$$

When $E < 0$ this represents a rate of fluid loss; $E > 0$ represents a rate of fluid gain. This type of equation has been studied in the context of condensation and evaporation in [28–31] and for small rain droplets in [24]. For flow into a porous substrate Equation (18) will be valid when the velocities $u, v \ll 1$ at the porous boundary $z = 0$; see [32]. For incoming droplets Equation (18) holds when the droplets are small and the droplet momentum is significantly less than the film momentum. If $h < k$, the velocities and flux are obtained in a similar manner as above, namely by integrating (3), (4) with $0 \leq z \leq h$ subject to (13). Theoretically this is a simple exercise and of practical interest; however, no experimental data has been found to verify this regime and so the following work will focus only on situations where $k < h$.

3. Limiting cases

In this section the limiting velocity profiles will be investigated for the three physically interesting limits, namely, when the resistance is large and small and when the roughness height is small. In the first case, $\omega \to \infty$, the flow below $z = k$ will be extremely slow and therefore the majority of fluid must flow above this region. When $\omega \to 0$, the fluid velocity above and below $z = k$ will approximate the classical parabolic profile. When $k \to 0$, there will be a small amount of flow below $z = k$ and the majority of the fluid will again flow with a parabolic velocity profile. In Sections 3.4, 3.5 bounds will be found for the steady-state film height and the limiting expressions used to determine approximate expressions for the coefficient K in Equation (2) and the correction factor $\beta = u_a/u_m$.

3.1. LARGE-RESISTANCE LIMIT

Simply substituting $\omega \to \infty$ in the expression for u_1 shows that $u_1 \sim \Lambda_1/\omega^2 + \mathcal{O}(\omega^{-3})$, provided $k \gg \omega^{-1}$. This will hold over most of the domain. In the vicinity of the transition region, $z \in [k - \zeta/\omega, k]$, (where $\zeta = \omega(k - z)$ is the scaled co-ordinate in the vicinity of $z = k$), a further term becomes important, *viz.*

$$u_1 = -\frac{\Lambda_1}{\omega}(k - h)\exp(-\zeta) + \frac{\Lambda_1}{\omega^2} + \mathcal{O}(\omega^{-3}). \tag{19}$$

Above $z = k$:

$$u_2 = -\frac{\Lambda_1}{2}(z - k)(z - k - 2(h - k)) - \frac{\Lambda_1}{\omega}(k - h) + \frac{\Lambda_1}{\omega^2} + \mathcal{O}(\omega^{-3}). \tag{20}$$

So, when $\omega \to \infty$, the velocity over most of the region $z < k$ is $\mathcal{O}(\omega^{-2})$. Just below the transition region, $z \to k^-$, an additional term becomes important and the velocity increases to $\mathcal{O}(\omega^{-1})$. This matches the velocity as $z \to k^+$ given by Equation (20). The leading-order velocity above the transition is exactly that which would occur on a smooth solid surface located at $z = k$. The higher-order corrections account for the fact that the fluid velocity at the transition point, at $\mathcal{O}(\omega^{-1})$, is non-zero.

3.2. SMALL-RESISTANCE LIMIT

In the limit of small resistance $\omega \to 0$ the velocity becomes

$$u_1 = -\frac{\Lambda_1}{2}z(z - 2h) - \frac{\Lambda_1}{24}\left[z^4 - 4hz^3 - 4k^3z + 12hk^2z\right]\omega^2 + \mathcal{O}(\omega^4) \tag{21}$$

$$u_2 = -\frac{\Lambda_1}{2}z(z - 2h) - \frac{\Lambda_1 k^3}{24}[8h - 3k]\omega^2 + \mathcal{O}(\omega^4). \tag{22}$$

To leading order in ω the velocities $u_1 = u_2$ are the classical expressions for flow on a smooth surface. The difference only occurs at $\mathcal{O}(\omega^2)$ where u_1 has a retarding term (provided $h > k$) with a quartic variation in z. The value of the retarding function increases from zero at the substrate to a constant value at $z = k$ which matches the constant at $\mathcal{O}(\omega^2)$ in u_2.

3.3. SMALL ROUGHNESS LIMIT

When $k \to 0$, the velocity is

$$u_1 = \frac{\Lambda_1}{\omega^2}(1 - \cosh(\omega z) + \omega h \sinh(\omega z)) - \frac{\Lambda_1 \omega h}{2}\sinh(\omega z)k^2 + \mathcal{O}(k^3), \tag{23}$$

$$u_2 = -\frac{\Lambda_1}{2}z(z - 2h) + \mathcal{O}(k^3). \tag{24}$$

In fact, since the u_1 expression holds for $z \le k$, the first term in u_1 is strictly $\mathcal{O}(k)$ and the second is $\mathcal{O}(k^3)$. As expected, above $z = k$ the parabolic velocity profile is retrieved. At the interface the velocity is of the order of the roughness height, $u_1 = u_2 = \Lambda_1 hk + \mathcal{O}(k^2)$.

The slip coefficient model of Miksis and Davis [16] leads to a velocity profile

$$u_{MD} = -\frac{\Lambda_1}{2}\left(z^2 + 2h(\alpha - z)\right). \tag{25}$$
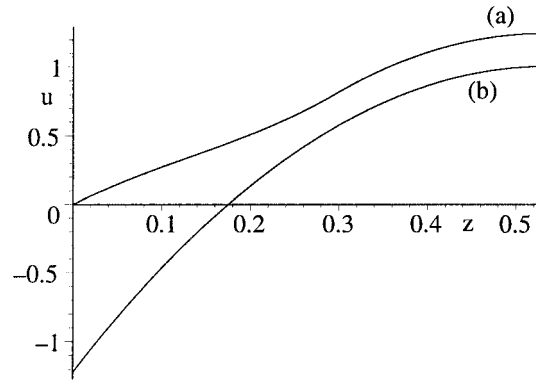
Figure 2. Comparison of velocity profiles predicted by (a) Equation (15) and (b) Equation (25)

This is valid for small surface roughness $k/h \ll 1$. The slip coefficient α is stated to be the average amplitude of the roughness height. Taking $\alpha = k/2$ means that Equations (24) and (25) only agree to leading order. The next non-zero term in (24) is $-\Lambda_1 \omega^2 h k^3/3$. Taking $\alpha = \omega^2 k^3/3$ forces the two velocity expressions to agree to $\mathcal{O}(k^3)$. Further, the slip coefficient now depends on the resistance caused by the substrate as well as the roughness height. This seems a more plausible situation, since the fluid flow must depend on the density of obstacles and their microscale roughness and not simply the average amplitude.

In Figure 2 the velocity profiles predicted by the current theory, Equations (15), and the model for flow over small surface roughness of Miksis and Davis, (25), are compared. The conditions correspond to one of the experimental cases given in Table 1, where $\mathrm{Re} = 145$. Curve (a) shows the fluid velocity predicted by the current method, with h set to the experimental value $h = 0.5325$ and $\omega = 6.7$ (this is determined in Section 5 to be the appropriate roughness coefficient for the surface). It can be seen that the fluid velocity increases monotonically from zero at the substrate to a maximum value $u(h) = 1.24$. The maximum velocity measured in the experiment is $u_e = 1.19$, hence the current method leads to an error of 4.6%. Curve (b) is the velocity predicted by Equation (25) with $\alpha = k/2 = 0.146$. The maximum velocity is $u_{MD}(h) = 1.0$, which is a 15.7% error. The velocity decreases monotonically from this value and becomes negative when $z < 0.175$, at the substrate $u(0) = -1.22$. This velocity profile is clearly physically unrealistic indicating that Equation (25) is inappropriate for predicting the velocity over a surface with significant roughness.

3.4.   BOUNDS ON THE FILM HEIGHT

For unidirectional flow in the steady-state the film height is determined by integrating (18),

$$Q_x = Ex + Q_i \tag{26}$$

where Q_i is the initial flux and Q_x is given by Equation (17). Taking the small ω expansion of (17) and rearranging gives the film height approximation when $h > k$

$$h = h_0 + \Lambda_1 k^3 \left[-\frac{k^2}{20} + \frac{kh}{4} - \frac{h_0^2}{3} \right] \omega^2 + \mathcal{O}(\omega^3), \tag{27}$$

where $h_0 = (3(Ex + Q_i)/\Lambda_1)^{1/3}$. For small k the same leading-order height, h_0, is obtained. For large ω

$$h = h_0 + k - \tanh(\omega k)\omega^{-1} + \mathcal{O}(\omega^{-2}). \tag{28}$$

Taking the leading-order expressions for the flux for these limiting cases shows the steady-state film height for unidirectional flow on a rough surface varies between

$$\sqrt[3]{\frac{3(Ex + Q_i)}{\Lambda_1}} \leq h \leq k + \sqrt[3]{\frac{3(Ex + Q_i)}{\Lambda_1}}. \tag{29}$$

The lower bound is the standard height predicted for flow on a smooth surface. The upper bound shows that on a very rough surface the height is simply the sum of the roughness height and h_0. This demonstrates that when the roughness is large the fluid flows above the rough region and the substrate effectively becomes $z = k$. In [24] it is shown that (when $E = 0$) the film heights generated by the saline technique described in [23] fall outside of this range, thus proving that the saline technique is not appropriate for laminar flow. All the laminar results of Phelps [7] and Woo and Brater [8] (who do not use the saline technique) lie within this range, except for a single result which is most likely incorrect and is discussed in more detail in Section 5.

3.5. Approximate expressions for K and β

In the introduction it was mentioned that the average velocity u_a is frequently approximated by Equation (2). In non-dimensional form this is

$$u_a = \frac{8h^2 \sin \theta}{K}. \tag{30}$$

On a smooth surface $K = 24$; experiments show that K increases with increasing roughness. However, as pointed out in [22], the functional dependence of K is unknown and therefore (30), is impractical for predicting the average velocity.

In the limit of small roughness $k \to 0$ the average velocity is given by

$$u_a = \frac{Q_x}{h} = \frac{\Lambda_1}{3} \left[h^2 + \omega^2 hk^3\right] + \mathcal{O}(k^4). \tag{31}$$

When gravity drives the flow down the surface $\Lambda_1 \approx -g_1 = \sin \theta$, where θ is the angle of inclination of the surface to the horizontal. Comparison of Equations (30) and (31) shows that, when the roughness height is small, the correct functional dependence for K is

$$K = 24 \left(1 - \frac{\omega^2 k^3}{h}\right) + \mathcal{O}(k^4). \tag{32}$$

Hence the correction to K is $\mathcal{O}(k^3)$ when the roughness height is small. Provided ω is not too large $(\omega^2 \ll h/k^3)$, taking $K = 24$ will therefore provide a good approximation when $k \ll 1$. The small ω expansion leads to a deviation from 24 only at $\mathcal{O}(\omega^2)$

$$K = 24 + \frac{6}{5} \frac{k^3 \left(3 k^2 - 15 kh + 20 h^2\right)}{h^3} \omega^2 + \mathcal{O}\left(\omega^3\right). \tag{33}$$

In the limit of large ω the current theory predicts

$$K = 24 \left(1 - \frac{k}{h}\right)^{-3} - \frac{72 \tanh(\omega k)}{\omega h} \left(1 - \frac{k}{h}\right)^{-4} + \mathcal{O}(\omega^{-2}). \tag{34}$$

The above equations provide explicit expressions for the functional dependence of K. K can be seen to depend on both the roughness and film heights. In the experimental situations discussed in the following section $\omega \sim 7$, for which Equation (34) is the appropriate limit (in fact this approximation is valid for $\omega \gg 3$). In agreement with experimental results, for a fixed film height, Equation (34) shows that K is an increasing function of the surface roughness; see [21]. For a fixed roughness height K decreases with the film height.

The correction factor discussed in the introduction, $u_a = \beta u_m$, has been found in experimental studies to vary between 0·2 and 0·65 for laminar flow, depending on the surface and flow conditions, see for example, [3, 5, 7, 23, 25, 26]. The maximum velocity, u_m, occurs at the free surface and is determined by substituting $z = h$ in Equation (15). The average velocity is simply the flux, defined by Equation (17), divided by the height. The correction factor may therefore be determined explicity from $\beta = Q_x/(u_m h)$. For large ω the correction factor turns out to be

$$\beta = \frac{u_a}{u_m} = \frac{2}{3}\left(1 - \frac{k}{h}\right)\left[1 + \frac{\tanh(\omega k)}{\omega}h\left(1 - \frac{k}{h}\right)^{-1}\right] + \mathcal{O}(\omega^{-2}). \tag{35}$$

The leading-order term indicates that for large ω the correction factor $\beta \in [0, 2/3]$ for $k \in [0, h]$ in accordance with the experimental data. Obviously, the theory is questionable when the roughness height is approximately the same as the film height and so the lower bound may be inaccurate. For small ω

$$\beta = \frac{2}{3} - \frac{1}{90}\frac{k^3\left(9\,k^2 - 30\,kh + 20\,h^2\right)}{h^3}\omega^2 + O\left(\omega^3\right). \tag{36}$$

The $\mathcal{O}(\omega^2)$ correction is negative until $k = 0.92h$. This indicates again that $\beta \leq 2/3$ over most of the acceptable range, but as the roughness height increases above 0·92 h the validity of results is questionable. This provides another reason for focussing on flows where $k < h$. For small k the correction factor deviates from 2/3 only at order k^3 and is always below this value:

$$\beta = \frac{2}{3} - \frac{2}{9}\frac{\omega^2}{h}k^3 + \mathcal{O}(k^4). \tag{37}$$

4. Unsteady analysis

4.1. SOLUTION BY THE METHOD OF CHARACTERISTICS

The two-dimensional form of Equation (18) may be written as

$$\frac{\partial h}{\partial t} + p(h)\frac{\partial h}{\partial x} = E, \tag{38}$$

where

$$p(h) = \frac{\Lambda_1}{\omega^2 C}\left[\{(2 + \omega^2 k^2)C - 2\omega k S - 2\} - 2(\omega^2 kC - \omega S)h + \omega^2 Ch^2\right]$$

and $C = \cosh(\omega k)$, $S = \sinh(\omega k)$. Equation (38) is quasilinear and may be solved by the method of characteristics. For an initially flat film, with height h_i, a particle at position (x_i, h_i) at $t = 0$ will subsequently have position
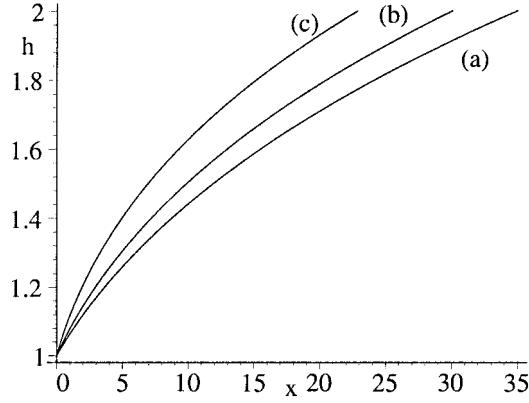
Figure 3. Comparison of film heights for (a) $\omega \to 0$, (b) $\omega = 5$ and (c) $\omega \to \infty$.

$$h = h_i + Et, \tag{39}$$

$$x = x_i + \frac{\Lambda_1}{E\omega^2 C}\left[\left\{(2 + \omega^2 k^2)C - 2\omega k S - 2\right\}(h - h_i) - (\omega^2 k C - \omega S)(h^2 - h_i^2)\right.$$
$$\left. + \frac{1}{3}\omega^2 C(h^3 - h_i^3)\right]. \tag{40}$$

This solution holds for all x and t.

In the limit of small ω (or small k) the particle height equation is unaffected, the leading-order x co-ordinate is

$$x = x_i + \frac{\Lambda_1}{3E}(h^3 - h_i^3). \tag{41}$$

Similarly, in the limit of large ω the leading order x-coordinate is

$$x = x_i + \frac{\Lambda_1}{3E}((h - k)^3 - (h_i - k)^3). \tag{42}$$

In Figure 3 three curves are shown. These represent the progress of a particle initially at $(x_i, h_i) = (0, 1)$ when $\Lambda_1 = 1 \cdot 5, E = 0.1, k = 0 \cdot 3$ for $t \in [0, 10]$. Curve (a) represents the small ω limit of Equation (41), curve (b) is the $\omega = 5$ result and curve (c) is the large ω result. When the resistance is small, the fluid particle moves rapidly down the slope and, in this scenario, ends at $x \approx 35$. As the resistance increases, the particle moves more slowly, hence the curve for large ω ends at $x \approx 23$. The final height is the same in all three cases. However, by the time the fluid particle in curve (c) has reached $x = 35$, it will be at height $h = 2 \cdot 24$. This gain in height is necessary to maintain the same flux since the resistance slows the flow rate.

4.2. LINEAR STABILITY

In the absence of resistance it is well known that flow driven solely by gravity on the surface of a smooth plane is stable to linear perturbations for all values of the wave number. The same is true in the current situation. If we look for solutions to (38) of the form

$$h = h_0(t) + h_1(t)e^{i\alpha x}, \tag{43}$$

where $h_1 \ll h_0$, the base state is $h_0 = Et + h_i$ and h_i is the initial film height. The perturbation h_1 is specified by

$$h_1 = A \exp\left(-i\alpha P(h_0)\right), \tag{44}$$

where

$$P(h_0) = \int P(h_0)\mathrm{d}t = \frac{\Lambda_1}{\omega^2 \cosh(\omega k)} \left[\left\{(2 + \omega^2 k^2)\cosh(\omega k) - 2\omega k \sinh(\omega k) - 2\right\}t + \right.$$
$$\left. \frac{\omega \sinh(\omega k) - \omega^2 k \cosh(\omega k)}{E}\left((h_i + Et)^2 - h_i^2\right) + \frac{\omega^2 \cosh(\omega k)}{3E}\left((h_i + Et)^3 - h_i^3\right)\right]. \tag{45}$$

Hence waves are propagated down the slope and the film is stable to linear perturbations. When the system loses mass, $E < 0$, the wave speed decreases with time. When $E > 0$, the wave speed increases with time. In the limit $E = 0$ the wave speed is constant; further, allowing $\omega \to 0$ provides the classic solution

$$h = h_0 + A \exp\left(i\alpha(x - \Lambda_1 h_i^2 t)\right). \tag{46}$$

Of course, perturbing the film will introduce non-negligible curvature and hence surface tension effects. Including surface tension into the model leads to

$$h = h_0 + A \exp\left(i\alpha(x - F(h_0)) - Ch_0^3\alpha^4 t\right), \tag{47}$$

where C is the inverse capillary number. Unlike gravity, which propagates the wave, surface tension acts to reduce the wave height and therefore stabilises the film.

5. Model validation

In all of the following examples the height-scale $H = 4$mm and the velocity scale $U = 10$cm/s. A series of experiments for uni-directional, steady laminar flow is described in Phelps [7]. The problem is therefore described mathematically by $Q_x = Q_i$, where Q_x is specified by Equation (17) and Q_i is measured. No fluid is lost or gained at the substrate or free surface so $E = 0$. The rough surface was prepared by attaching spherical particles of diameter $1 \cdot 17$mm onto a nominally smooth surface (the non-dimensional roughness height is therefore $k = 0 \cdot 2925$). Water was then poured down the slope at a rate Q_i. Table 1 contains a summary of the experimental results where the maximum velocity was measured. The columns show the Reynolds number, the gravity term Λ_1, the measured height h_e, the value of ω obtained by solving Equation (17) with $h = h_e$, the measured maximum velocity u_{me}, the maximum velocity u_m, (obtained by substituting for Λ_1, k, ω and setting $z = h$ in Equation (15)) and the percentage difference $100(u_m - u_{me})/u_{me}$. The Reynolds number quoted in Table 1 is slightly different to that quoted by Phelps. It seems likely that Phelps uses the formula $\text{Re} = u_a h/\nu$ since, if the simpler formula $\text{Re} = Q_i/\nu$ is used, this indicates that the viscosity ν varies between $6 \cdot 8 \times 10^{-7}$ and $9 \cdot 6 \times 10^{-7}$m^2/s. The fluid viscosity is unlikely to change this much during the experiments, hence the Reynolds number given in Table 1 is calculated using $\text{Re} = Q_i/\nu$, where Q_i is the flux quoted by Phelps and ν is taken as 10^{-6}m^2/s.

With the exception of the first result the agreement is extremely good. It seems likely that some error has occurred in obtaining this first result, since it appears as an outlier in the full table of experimental data in Phelps. Further, of the 30 results presented by Phelps,

Table 1. Comparison of predicted maximum velocity with experimental value.

Re	Λ_1	h_e	ω	u_{me}	u_m	% error
34	1·30	0·565	0·01	0·256	0·220	−14·2
34	0·75	0·8375	7·2	0·165	0·178	7·9
84	0·75	1·08	6·8	0·305	0·329	8·0
142	0·75	1·2575	6·5	0·451	0·469	4·1
145	15·68	0·5325	7·0	1·189	1·214	2·1
314	7·18	0·825	6·95	1·661	1·660	−0·04
390	3·73	1·06	6·83	1·561	1·562	0·07
466	2·41	1·25	5·75	1·475	1·529	3·7

where Re $\leq$ 500, this is the only one where the film height falls outside the bounds given by Equation (29). In general, the % error is worst at low flow rates. This may be partially explained by the measurement technique. To determine velocity profiles Phelps introduced spherical aluminium particles, with diameter d =0·025mm, into the flow. The maximum rate at which these particles will sink is determined by the balance between gravity and viscous resistance,

$$u_s \approx \frac{1}{18} d^2 \frac{\rho_a - \rho_w}{\mu} g,$$

where ρ_a and ρ_w are the particle and water density and μ is the dynamic viscosity. Substituting the appropriate values leads to $u_s \approx 0.58$mm/s. Now consider a film of height 2mm flowing over a smooth surface with a maximum velocity of 3cm/s. If the particles are introduced 5cm above the measuring point, the maximum distance they will drop below the surface when they reach the measuring point is 0·97mm. At this depth the velocity is 2·3cm/s and the measurement error is therefore of the order 25%. The error will rapidly decrease as the velocity increases. For example, with a maximum velocity of 10cm/s the error drops to 2·5%. It is therefore not surprising that the agreement between the current theory and the experimental results improves as the velocity increases. Of course this statement only holds in the laminar regime, below Re = 500. The final result, with Re = 466, is approaching this transition and so shows a slight increase in the error. It is likely that this error will continue to increase until the transition value is reached, at which point the theory is no longer valid.

Neglecting the first result, the average value for ω is 6·7. Employing this value to calculate the maximum velocity leads to an error of less than 1% in all cases when compared to the value of u_m given in Table 1. It may therefore be deduced that $\omega = 6.7$ is a good estimate for the resistance coefficient of this particular surface. In fact, it appears that the result is not very sensitive to the choice of ω. For example, in the case Re = 84, substituting for h and k in Equation (15) (while setting $z = h$ to provide the maximum velocity), varying ω by a factor of 2, from 4 to 8 leads to only a 16% change in the maximum velocity prediction. Practically this means that just a few experiments could be carried out to determine ω and hence describe a given surface.

Finally, Phelps [7, Figure 7] shows a set of three experimental pictures for the velocity profile through the film for flow above, near to and far from a roughness element. The experi-
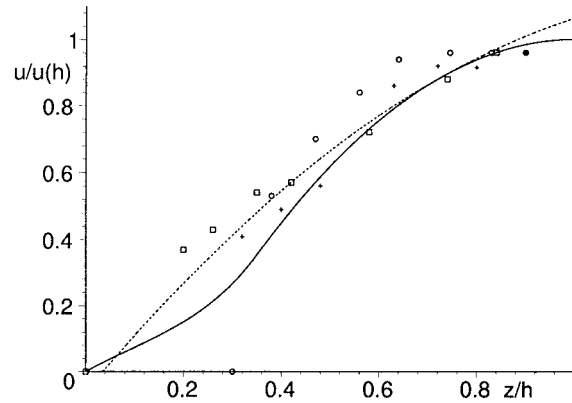
Figure 4. Comparison of theoretical, Equation (15), (solid line) and experimental velocity profiles [7] (data points) and a least-squares fit to the experiments (dashed line)

mental data for the results labelled test 1 are shown in Figure 4. The circles show the velocity measured above an element, note that the velocity is zero on top of the element, $z = 0.2925$. The crosses represent flow near to the element and the squares flow far away from the element. The squares lie approximately on the quadratic curve defined by Equation (24). The dashed line is a least-squares fit of all the data points to a quadratic curve. Above $z = 0.4$ the data points are all close to the dashed line. Below this value there is a greater spread in the data. The data represented by the circles shows that the velocity reaches zero at $z = 0.2925$. The squares show the velocity reaching zero at $z = 0$. The cross data points lie between these values. The solid line is the curve predicted by Equation (15). For $z > 0.5$ it lies close to the least-squares approximation. Below this value it decreases more rapidly. This is due to the fact that it is an average of the velocities and must account for the zero velocity near the roughness height. The closeness of the solid curve to the data points above the roughness and the fact that it lies between the data points below the roughness height indicates that the current approach does indeed provide a reasonable approximation for the average flow characteristics.

6. Conclusions

A method has been developed for three-dimensional laminar thin film flow on a rough substrate. Three physically interesting limits to the model have been investigated for uni-directional flow and used to provide simple expressions for the velocity, bounds on the film height, the coefficient K and the correction factor β. The unsteady model was analysed and a solution found by the method of characteristics. The governing equation was also shown to be stable to linear perturbations.

It has been shown that for large ω the empirical formula for average velocity, (2), can provide a reasonable approximation. The previous drawback to this formula was the undetermined variable K. The current work provides an expression for K and shows that as ω decreases the simple form of Equation (2) is no longer appropriate. However, in the limit $\omega \to 0$ the formula will once again be valid. An explicit formula has also been given for the correction factor β. For laminar flow $\beta = 2/3$. For flow over a rough surface the current method shows $\beta \in (0, 2/3]$ in agreement with experimental results.

Comparison with experimental data shows that the predictions for the velocity profile are very good. The worst agreement occurs at low fluid velocities, when the experimental

measurements are most likely to be inaccurate. The velocity profile through the film also shows good qualitative agreement with the average of a series of velocity profiles obtained experimentally.

The model involves one unknown parameter, ω, which quantifies the resistance of the surface to the flow. This parameter arises through the assumption that the resistance can be approximated by a linear form. The value of ω cannot be determined from the model and therefore at least one steady-state, unidirectional experimental result is required. Measuring Q and h and substituting the values in the flux expression (17) provides an equation to determine ω (which must be solved numerically). Alternatively, if the maximum velocity and h are measured, then solving (15), after substituting $z = h$, determines ω. This was the method employed in Section 5. If the film height is difficult to measure accurately, the maximum velocity and flux may be measured and then (17) and (15) (again with $z = h$) may be solved simultaneously to determine the height and roughness coefficient. Numerical tests indicate that the velocity profile is not very sensitive to the choice of ω. The method is therefore quite robust for practical applications. However, it is still sensible to carry out a number of experiments and find an average value for ω.

Whilst the model appears to work well for the types of flow considered in this paper, its use will be limited in practical situations. In the future it is intended to develop the model along the following lines:

- allow for non-negligible velocity at the substrate,
- allow for the effect of rain on the momentum balance,
- incorporate substrate erosion and particle transport,
- investigate models where $k > h$.
- relate ω to the various other measures of surface roughness.

In this way it is hoped to provide a practical tool for modelling overland fluid flow.

Acknowledgements

References

1. V.T. Chow, *Open Channel Hydraulics*. New York: McGraw-Hill, (1959) 680pp.
2. A.D. Abrahams, A.J. Parsons and S.-H. Luk, Field measurement of the velocity of overland flow using dye tracing. *Earth Surf. Proc. Landforms* 11 (1986) 653–657.
3. S.H. Luk and W. Merz, Use of the salt tracing technique to determine the velocity of overland flow. *Soil Technology* 5 (1992) 289–301.
4. D.S.L. Lawrence, Macroscale surface roughness and frictional resistance in overland flow. *Earth Surf. Proc. Landforms* 22 (1997) 365–382.
5. G. Li, A.D. Abrahams and J.F. Atkinson, Correction factors in the determination of mean velocity of overland flow. *Earth Surf. Proc. Landforms* 21 (1996) 509–515.
6. J.M. Roels, Flow resistance in concentrated overland flow on rough surfaces. *Earth Surf. Proc. and Landforms* 9 (1984) 541–551.
7. H.O. Phelps, Shallow laminar flows over rough granular surfaces. *J. Hydraulics Division ASCE* HY3 101 (1975) 367–384.

8. D-C Woo and E.F. Brater, Laminar flow in rough rectangular channels. *J. Geophys. Res.* 66 (1961) 4207–4217.

9. B.T. Guy, W.T. Dickinson, R.P. Rudra and G.J. Wall, Hydraulics of sediment-laden sheetflow and the influence of simulated rainfall. *Earth Surf. Proc. Landforms* 15 (1990) 101–118.

10. D.S.L. Lawrence, Hydraulic resistance in overland flow during partial and marginal surface inundation: experimental observations and modelling. *Water Resources Res.* 36 (2000) 2381–2393.

11. E.P. Lozowski, K. Szilder and L. Makkonen, Computer simulation of marine ice accretion. *Phil. Trans. R. Soc. London* A 358 (2000) 2811–2845.

12. R.W. Gent, N.P. Dart and J.T. Cansdale, Aircraft icing. *Phil. Trans. R. Soc. London* A 358 (2000) 2873–2911.

13. T.G. Myers, J.P.F., Charpin and C.P. Thompson, slowly accreting glaze ice due to supercooled droplets impacting on a cold substrate. *Phys. Fluids* 14 (2002) 240–256.

14. A. Defina, Two-dimensional shallow flow equations for partially dry areas. *Water Resources Res.* 36 (2000) 3251–3264.

15. J.S. Kim, S. Kim and F. Ma, Topographic effect of surface roughness on thin-film flow. *J. Appl. Phys.* 73 (1993) 422–428.

16. M.J. Miksis and S.H. Davis, Slip over rough and coated surfaces. *J. Fluid Mech.* 273 (1994) 125–139.

17. P. Neogi and C.A. Miller, Spreading kinetics of a drop on a rough solid surface. *J. Colloid Inter. Sci.* 92 (1983) 338–349.

18. R.I. Bowles, Upstream influence and the form of standing hydraulic jumps in liquid-layer flows on favourable slopes. *J. Fluid Mech* 284 (1994) 63–96.

19. W.G. Pritchard, L.R. Scott and S.J. Taverner, Numerical and asymptotic methods for certain viscous free-surface flows. *Phil. Trans. R. Soc. London* A340 (1992) 1–45.

20. R.E. Horton, H.R. Leach and R. Van Vliet, Laminar sheet flow. *Trans. American Geophys. Union* 2 (1934) 393–404.

21. D.M. Katz, F.J. Watts and E.R. Burroughs, Effects of surface roughness and rainfall impact on overland flow. *J. Hydraulic Engng.* 121 (1995) 546–553.

22. H. Rouhipour, C.W. Rose, B. Yu and H. Ghadiri, Roughness coefficients and velocity estimation in well-inundated sheet and rilled overland low without strongly eroding bed forms. *Earth Surf. Proc. Landforms* 24 (1999) 233–245.

23. G. Li and A.D. Abrahams, Effect of saltating sediment load on the determination of the mean velocity of overland flow. *Water Resources Research* 33 (1997) 341–347.

24. T.G. Myers, Modelling laminar sheet flow over rough surfaces. *Water Resources Research* 38(11), 1230, DOI: 10.1029/2000WR000154, (2002).

25. W.W. Emmett, *The Hydraulics of Overland Flow on Hillslopes*. US Geological Survey Professional Paper, 662-A (1970).

26. A.D. Abrahams, and G. Li, Effect of saltating sediment on flow resistance and bed roughness in overland flow. *Earth Surface Processes Landforms 23* (1998) 953–960.

27. T.G. Myers, Surface tension driven thin film flows. *Siam Rev.* 40 (1998) 441–462.

28. T.G. Myers, J.P.F. Charpin and S.J. Chapman, The flow and solidification of a thin fluid film on a arbitrary three-dimensional surface. *Phys. Fluids* 14 (2002) 2788-2803.

29. B. Reisfeld, S.G. Bankoff and S.H. Davis, The dynamics and stability of thin liquid films during spin coating. I. Films with constant rates of evaporation or absorption. *J. Appl. Phys.* 70 (1991) 5258–5266.

30. J.P. Burelbach, S.G. Bankoff and S.H. Davis, Non-linear stability of evaporating/condensing liquid films. *J. Fluid Mech.* 195 (1988) 463–494.

31. S.D. Howison, J.A. Moriarty, J.R. Ockendon, E.L. Terrill and S.K. Wilson, A mathematical model for drying paint layers. *J. Engng. Math.* 32 (1997) 377–394.

32. P.G. Saffman, On the boundary condition at the surface of a porous medium. *Stud. Appl. Math.* 50 (1971) 93–101.

33. T.S.W. Wong and C-N Chen, Time of concentration formula for sheet flow of varying flow regime. *J. Hydrologic Engng.* 123 (1997) 136–139.